

ARTICLE

Effect of Catalyst Concentration on the Properties of Bio-based Epoxy Vitrimer with Dynamically Adaptive Networks[†]

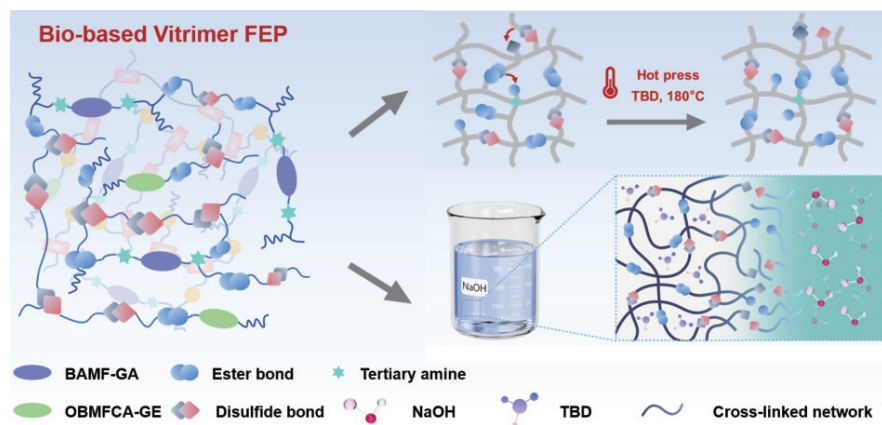
Wenyan Zhang^{a‡}, Yuting Chu^{b‡}, Chuang Li^{b*}, Yao Fu^{a*}

a. Key Laboratory of Precision and Intelligent Chemistry, Anhui Province Key Laboratory of Biomass Chemistry, University of Science and Technology of China, Hefei 230026, China

b. Institute of Advanced Technology, University of Science and Technology of China, Hefei 230000, China

(Dated: Received on December 2, 2025; Accepted on December 25, 2025)

Epoxy resins are widely employed in wind turbine blades, drone rotors, and automotive interiors due to their excellent mechanical properties and long



service life. However, their insoluble and infusible cross-linked networks pose a significant recycling challenge, particularly with the impending retirement of the first generation of wind turbine blades. In this work, we reported a fully bio-based epoxy Vitrimer (FEP) incorporating a dual-dynamic covalent network design and systematically investigated the influence of the 1,5,7-triazabicyclo[4.4.0]dec-5-ene (TBD) catalyst on its curing kinetics, thermal/mechanical properties, dynamic exchange behavior, and degradation performance in a mild alkaline solution. Compared to conventional epoxy resins, FEP exhibited superior tensile strength and elongation at break at an optimal TBD concentration (2 wt%), achieving an excellent strength-toughness balance. The presence of TBD accelerated the exchange rates of both disulfide and ester bonds, endowing FEP with notable stress relaxation at elevated temperatures. Moreover, FEP demonstrated complete dissolution in 1 mol/L NaOH within 6 h at 25 °C. These results underscored the exceptional strength, toughness, and recyclability of FEP, positioning it as a promising, environmentally friendly matrix resin for next-generation applications in the new energy sector.

Key words: Bio-based materials, Epoxy Vitrimer, Catalyst concentration, Dynamically adaptive networks

I. INTRODUCTION

Owing to high cross-linking density and excellent stability, epoxy thermosets (EPTs) are widely used in new energy fields such as wind turbine blades and automotive interiors [1]. However, their dense three-dimensional network structure and chemical inertness make

[†] Part of Special Issue dedicated to Professor Qing-shi Zhu on the occasion of his 80th birthday.

[‡] These authors contributed equally to this work.

* Authors to whom correspondence should be addressed.

liuchuang@mail.ustc.edu.cn, fuyao@ustc.edu.cn

them notoriously difficult to recycle. The most common epoxy-amine cross-linked systems are not only constrained by reproductive toxicity concerns associated with bisphenol-A (BPA)-based epoxy monomers but also require harsh conditions for decomposition, conflicting with green and sustainable development goals. In this context, recyclable thermosets based on dynamic covalent adaptable networks (CANs) have emerged [2]. These materials incorporate reversible covalent bonds—such as ester, disulfide, imine, siloxane, and acetal linkages—into the polymer backbone, thereby conferring epoxy resins with recyclability, reprocessability, and self-healing capabilities [3–5]. In 2011, Leibler and co-workers proposed a novel class of remodelable tri-network epoxy-based glassy polymers, termed ‘Vitrimers’ [6]. These materials maintain the stability and heat resistance of conventional thermosets at room temperature, while their cross-linked networks can undergo topological rearrangement under elevated temperatures in the presence of a catalyst, enabling reprocessing and recycling. Despite these advantages, the development of Vitrimers still faces two critical challenges: 1) The introduction of dynamic covalent bonds often compromises mechanical performance due to the relatively weak nature of these bonds. 2) It remains difficult to simultaneously achieve high toughness and strength in Vitrimers, a common trade-off in engineering plastics.

In epoxy Vitrimer systems, catalyst concentration serves as a key factor regulating both the rate of dynamic exchange reactions and the macroscopic material properties. It influences the activation energy barrier of dynamic covalent bond exchange and the topology freezing transition temperature, and directly determines the material’s rheological behavior, mechanical performance, and degradation efficiency. For instance, Cui *et al.* [7] demonstrated that zinc-based catalysts significantly affected the curing behavior, thermal properties, mechanical performance, and dynamic self-healing capability of Vitrimers. A small amount of ZnAA (1%) accelerated the curing rate, whereas a higher concentration (>5%) led to a decrease in the storage modulus (E') at elevated temperatures, confirming the catalytic role of ZnAA in ester and disulfide exchange reactions. Thus, the mechanism by which catalyst concentration affects overall performance in different systems requires further investigation.

In recent years, recyclable epoxy systems derived from renewable biomass resources have shown promis-

ing prospects. For example, Wu *et al.* [8] reported a fully lignin-derived epoxy resin (DGF/MBCA) whose composites exhibit excellent thermomechanical properties and closed-loop recyclability. Wang *et al.* also reported a self-healing, recyclable, and degradable bio-based epoxy Vitrimer with dual dynamic imine and disulfide bonds, the core raw material of which, 5-hydroxymethylfurfural (HMF), is derived from carbohydrates [9]. Nevertheless, efficient structural reprocessing in these systems still relies on high temperatures and harsh catalytic conditions, underscoring that the selection and optimization of catalyst type and dosage remain critical for achieving green recycling in bio-based systems.

Herein, we designed a dual-dynamic network Vitrimer FEP employing furan-based bi-/tetra-functional epoxides as the rigid cross-linking skeleton and poly(thioctic acid) as the flexible dynamic chain segment, and systematically investigated the influence of catalyst concentration on curing kinetics, network evolution, mechanical properties, and recycling behavior. By modulating catalyst concentration, the exchange rates of ester and disulfide bonds were finely tuned to balance rigidity, toughness, and reprocessability. Furthermore, through green degradation and hot-pressing reshaping processes, we aimed to construct a fully bio-based, high-performance, and closed-loop recyclable epoxy Vitrimer suitable for large-scale composite applications such as wind turbine blades.

II. EXPERIMENTS

A. Reagents

2,5-Furyl dimethylamine (BAMF) and 5,5'-(oxybis(methylene))bis(furan-2-carbonyl chloride) (OBMFCA) were provided by Hefei Leaf Biotech Co., Ltd. Thioctic acid (TA) was purchased from Sigma Aldrich. Glycidol, epichlorohydrin (ECH), thionyl chloride, 1,5,7-triazabicyclo[4.4.0]dec-5-ene (TBD) and other chemicals were purchased from Aladdin.

B. Preparation of BAMF-GA

BAMF (0.2 mol, 1 equiv.), ECH (14 equiv.), and tetrahydrofuran (THF, 150 mL) were added into a 500 mL round-bottom flask and reacted at 30 °C overnight. Subsequently, a 30 wt% NaOH aqueous solution (12 equiv.) was added, and the reaction was continued at 45 °C for 6 h. After completion, the mixture was

extracted with ethyl acetate (EA, 500 mL). The product was purified by column chromatography with an EA/PE=1/3 eluent and identified as glycidyl amine by ^1H NMR spectroscopy. ^1H NMR (400 MHz, Chloroform-*d*) δ 7.20–7.17 (d, 2H), 6.53–6.46 (d, 2H), 4.66–4.54 (m, 6H), 4.18–4.09 (q, 4H), 3.36–3.30 (m, 2H), 2.93–2.87 (m, 2H), 2.75–2.69 (m, 2H).

C. Preparation of OBMFCA-GE

Glycidol (2.4 equiv.), triethylamine (2.4 equiv.), and dichloromethane (DCM, 50 mL) were added into a 500 mL round-bottom flask, and the mixture was reacted in an ice bath. OBMFCA (1 equiv.) was first dissolved in DCM (20 mL) and then slowly added to the mixture over 30 min. The reaction was stirred at room temperature for 4 h. After completion, the mixture was washed twice with a saturated sodium chloride solution. The organic phase was separated, dried over anhydrous Na_2SO_4 , filtered, and concentrated under reduced pressure to yield a white powder. The product was identified as glycidyl ester by ^1H NMR spectroscopy. ^1H NMR (400 MHz, Chloroform-*d*) δ 6.13–6.03 (m, 1H), 3.88–3.63 (q, 2H), 3.07–2.92 (m, 2H), 2.86–2.78 (m, 1H), 2.73–2.65 (m, 2H), 2.58–2.49 (m, 1H), 2.48–2.40 (m, 2H).

D. Preparation of FEP neat resin

In a typical experiment, poly(thiocetic acid) (PTA) was first synthesized via ring-opening polymerization of TA (30 mmol) at 140 °C for 0.5 h. Subsequently, a mixture of BAMF-GA (10 mmol) and OBMFCA-GE (10 mmol), and a catalytic amount of TBD (0–5 wt% relative to the total mass of epoxides) with varying stoichiometric ratios was rapidly introduced into the PTA melt at 70 °C. After mixing for 60 s, the homogeneous mixture was transferred to a PTFE mold and degassed under vacuum for 5 min to remove bubbles. The curing process consisted of pre-curing at 70 °C for 4 h followed by post-curing at 160 °C for 1 h, yielding a crimson-colored FEP Vitrimer.

E. Hot pressing process of FEP

The cured FEP samples were sectioned into pieces using a razor blade and placed into stainless steel fixtures. The samples were then remolded via hot pressing at 180 °C and 20 MPa for 1 h using a flat vulcanizer.

F. Chemical degradation of FEP

Chopped FEP (100 mg) was combined with 1 mol/L NaOH (20 mL) in a three-neck round-bottom flask equipped with a magnetic stirrer. The alkaline degradation reaction was conducted at room temperature for 6 h under continuous stirring. Following this, 1 mol/L HCl was added to the mixture and allowed to react for an additional 2 h, during which the mixture separated into distinct layers. The reaction mixture was then filtered to separate the products.

G. Chemical stability, swelling, and gel content testing

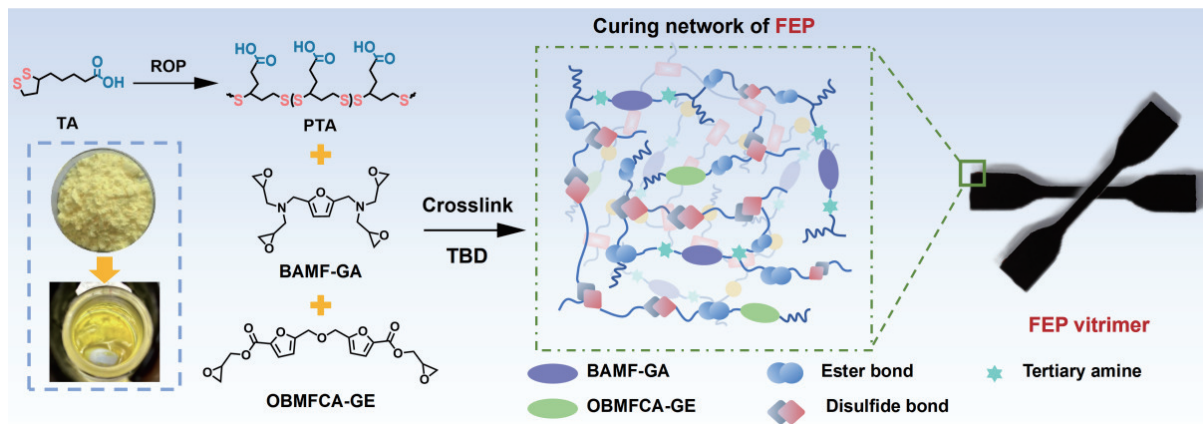
The swelling ratio was measured by immersing samples with five different TBD concentrations (~20 mg, m_0) in methanol at room temperature until equilibrium. Once swelling equilibrium was reached, the samples were removed from the solution, and any excess solvent on the surface was wiped off using filter paper. The swollen samples were then weighed (m_1), and the swelling ratio was calculated according to the following formulas:

$$\text{Gel content}(\%) = \frac{m_1}{m_0} \times 100\%$$

$$\text{Swelling ratio}(\%) = \frac{m_1 - m_0}{m_0} \times 100\%$$

H. Characterization

Proton nuclear magnetic resonance (^1H NMR) spectra were recorded on Bruker 400 MHz NMR spectrometer. Raman spectra of TA and FEP were recorded on a LabRAM HR Evolution (Horiba, Japan) over the range of 400–1000 cm^{-1} . Atomic force microscopy (AFM) phased images and height images were scanned on a Bruker Dimension Icon. The viscosity was tested on a SNB-4 rheometer (Shanghai YiXin) with a 25 mm diameter rotor. Non-isothermal differential scanning calorimetry (DSC) was tested to analyze the curing kinetics of FEP and heated at different heat rate (5, 10, 15, 20 $^{\circ}\text{C} \cdot \text{min}^{-1}$) over a temperature range from 30 °C to 300 °C. The apparent activation energy (E_a) of the curing reaction was determined using the Kissinger equation. This approach assumes the maximum reaction rate occurs at the exothermic peak temperature (T_p) and that the reaction order remains constant throughout the curing process. E_a was calculated according to Kissinger equation:



Scheme 1. Preparation route of FEP neat resin.

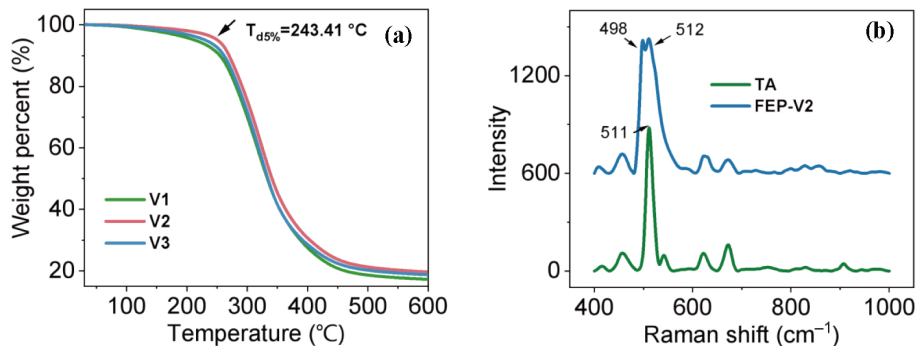


FIG. 1 Curing kinetics curves under different TBD concentration.

$$\ln \left(\frac{\beta}{T_p^2} \right) = \ln \left(\frac{AR}{E_a} \right) - \frac{E_a}{RT_p}$$

where R is the universal gas constant, A is the pre-exponential factor, β is the heating rate, and T_p is the temperature of the exothermic peak.

III. RESULTS AND DISCUSSION

A. Preparation of FEP neat resin

In this study, the epoxy Vitrimer FEP was synthesized using a two-step process (Scheme 1). First, the poly(thiocetic acid) (PTA) precursor was prepared via ring-opening polymerization of thioctic acid (TA). Subsequently, furan-based bifunctional epoxide (OBMFCA-GE) and furan-based tetrafunctional epoxide (BAMF-GA) were introduced into the system for curing. The curing procedure consisted of two stages: 4 h at 80 °C, followed by a final post-curing step at 160 °C for 1 h to ensure complete carboxyl-epoxy curing.

TA served as the curing agent in this system, with its most notable feature being the formation of linear PTA through ring-opening polymerization of the disulfide

bond in the five-membered ring [10]. However, the dynamic behavior of linear PTA at room temperature leads to spontaneous depolymerization, resulting in relatively low thermal stability and mechanical properties, which limits its application. Therefore, utilizing the carboxyl groups of TA as curing sites and incorporating the furan-based epoxy resin mixture as the cross-linking matrix represents an effective approach to enhance its thermal and mechanical performance. In this design, the tetrafunctional furan-based epoxide (BAMF-GA) was constructed as an inherently rigid structure containing a tertiary amine moiety, while the furan-based bifunctional epoxide (OBMFCA-GE) was designed with a more flexible architecture incorporating ether and ester linkages. This molecular design created a “rigid-flexible” synergistic system. Consequently, the three-component system (PTA/OBMFCA-GE/BAMF-GA) synergistically combined the flexibility and disulfide dynamics of PTA with the rigid, aromatic furan-based skeleton, enabling precise tuning of cross-linked density and dynamic exchange rates to achieve a balanced performance profile that would be difficult to attain with simpler two-component formulations.

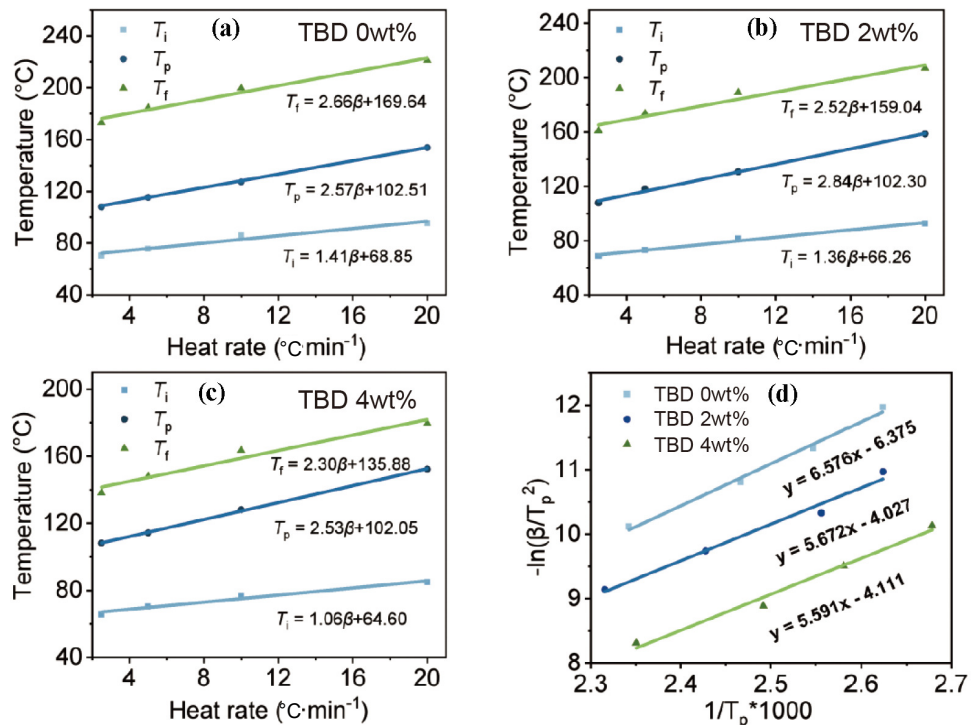


FIG. 2 (a-c) Non-isothermal DSC curves of FEP with TBD catalyst concentrations of (a) 0 wt%; (b) 2 wt%; (c) 4 wt%. (d) Linear fitting of $1/T_p - \ln(\beta/T_p^2)$ for different curing systems.

To investigate the influence of TA ring-opening polymerization on the properties of the FEP, experiments were conducted with different prepolymerization approaches, yielding FEP-V1 to FEP-V3. The thermal properties of FEP prepared with various prepolymerization strategies were monitored. Thermogravimetric Analysis (TGA, FIG. 1(a)) revealed that the thermal degradation curves of FEP-V1 to FEP-V3 exhibited similar trends, with the 5% thermal decomposition temperature of all samples exceeding 200 °C, indicating high thermal stability across the FEP series. Among them, FEP-V2 demonstrated the highest thermal decomposition temperature ($T_{d5\%} = 243.41$ °C), suggesting that ring-opening polymerization of TA with the catalyst at 140 °C resulted in superior thermal performance. This is attributed to the formation of a more uniform and stable PTA precursor under these conditions, which subsequently leads to a more homogeneous cross-linked network. Subsequently, Raman spectroscopy was performed on FEP-V2 to confirm the ring-opening polymerization of TA in FEP. The Raman spectrum (FIG. 1(b)) showed that the single absorption peak at 511 cm⁻¹, attributed to the S-S bond in TA, split into two peaks at 498 and 512 cm⁻¹ after curing, confirming the ring-opening polymerization of TA [11, 12]. The observed peak splitting is characteristic of

TABLE I Characteristic curing temperatures of FEP under different TBD concentrations.

TBD/wt%	$T_i/^\circ\text{C}$	$T_p/^\circ\text{C}$	$T_f/^\circ\text{C}$	$E_a/(\text{kJ}\cdot\text{mol}^{-1})$
0	68.65	102.51	169.64	54.67
2	66.26	102.30	159.04	47.16
4	64.60	102.05	135.88	46.48

the conformational change in the disulfide bond from a constrained ring structure to a more flexible linear polymeric form.

B. Curing kinetics and rheology analysis

As an ester exchange catalyst, TBD significantly influences the curing kinetics of FEP. Non-isothermal DSC provided characteristic curing temperatures—onset temperature (T_i), peak temperature (T_p), and termination temperature (T_f), at different TBD contents (Table I), thereby determining the suitable curing temperature for the system. The activation energy of the curing reaction under varying TBD concentrations was further calculated using the Kissinger equation (FIG. 2). As shown in Table I, the activation energy E_a decreases with increasing TBD content. However, when the TBD content rises from 2 wt% to 4 wt%, E_a only decreased by 0.68 kJ/mol, indicating that the ester exchange rate of the system has already reached its opti-

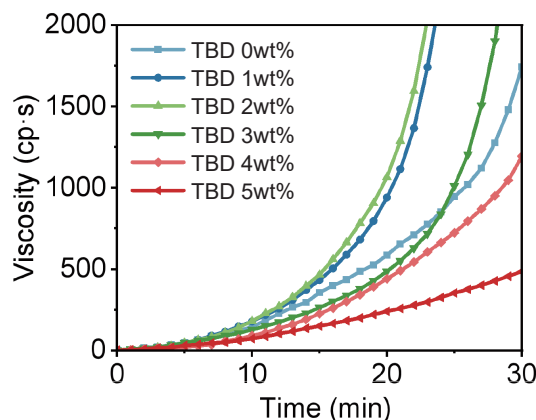


FIG. 3 Time-dependent viscosity during the curing process at 70 °C.

mal level at a TBD concentration of 2 wt%. This saturation effect suggests that beyond a certain concentration, additional TBD molecules do not further participate effectively in the rate-determining step of the transesterification, possibly due to aggregation or diffusion limitations within the increasingly viscous reaction medium, which is consistent with the subsequent rheological observations.

Based on the aforementioned curing kinetics analysis, the gel point temperature of FEP was determined to be approximately 70 °C (estimated from the T_i value). Consequently, the effect of TBD concentration on the viscosity of the FEP system was investigated at this temperature (FIG. 3). When TBD (1–2 wt%) was introduced, the viscosity of the system increased due to the accelerated formation of thiol radicals and ester bonds. However, upon further increasing the TBD concentration (> 2 wt%), the viscosity decreased, a phenomenon that corroborates the aforementioned analysis of catalyst saturation. This can be attributed to the excessive generation of active catalytic centers. An overabundance of catalytic sites may lead to an overly rapid initial gelation, creating a heterogeneous network with localized regions of high cross-link density and others that are under-cross-linked, ultimately reducing the overall viscosity buildup and potentially compromising the final network uniformity. Therefore, at a TBD concentration of 2 wt%, the curing rate of the system reached its maximum, further corroborating the reliability of the curing kinetics analysis.

C. Thermal and mechanical properties analysis

The cross-linked network of FEP incorporates dual dynamic covalent bonds: disulfide bonds and ester

bonds. As two types of dynamic covalent bonds with distinct degrees of reversibility, the bond energy of disulfide bonds is 251 kJ/mol, while that of the C–O bond in the ester group is 326 kJ/mol. Modulating the catalyst concentration affects the rate of transesterification, thereby regulating the polymerization process and significantly influencing the thermal and mechanical properties of the material. The concentration of TBD was varied within the range of 0–5 wt%. As the concentration increased, both the thermal decomposition temperature $T_{d5\%}$ and the glass transition temperature T_g exhibited peak values ($T_{d5\%}=243.41$ °C, $T_g=48.38$ °C) (FIG. 4(a, b)). The initial increase in $T_{d5\%}$ and T_g with TBD up to 2 wt% was due to the formation of a more complete and densely cross-linked network, while the subsequent decline at higher loadings was likely a consequence of network heterogeneity and the plasticizing effect of excess, unbound catalyst molecules.

As shown in FIG. 4(c), the tensile strength reached a maximum at 2 wt% TBD ($\sigma=64$ MPa), while the elongation at break consistently increased with rising TBD concentration. This trend can be attributed to the accelerated transesterification rate within the polymer network at higher TBD concentrations, which softens the material, reduces its strength, and consequently enhances elongation. The continuous increase in elongation suggests that the dynamic exchange activity promotes chain mobility and energy dissipation, even as the ultimate strength is optimized at a specific catalyst concentration. Notably, in addition to confirming the presence of peak values in storage modulus and glass transition temperature, FIG. 4(d) also revealed that all FEP samples exhibit dual glass transition temperatures. This phenomenon demonstrates a pronounced phase-separation effect in the FEP based on dual dynamic covalent bonds. The lower T_g is associated with the flexible, disulfide-rich PTA domains, while the higher T_g corresponds to the more rigid, furan-epoxy rich domains. This inherent phase separation was directly visualized by AFM phase and height images (FIG. 5), which clearly reveal the biphasic morphology. In this architecture, discrete soft domains were embedded in a continuous rigid matrix, which was essential for balancing toughness and stiffness. The soft regions dissipate mechanical energy, while the rigid percolating network maintained dimensional stability during dynamic exchange. This structural synergy thus married the dynamic bond-exchange chemistry with a damage-toler-

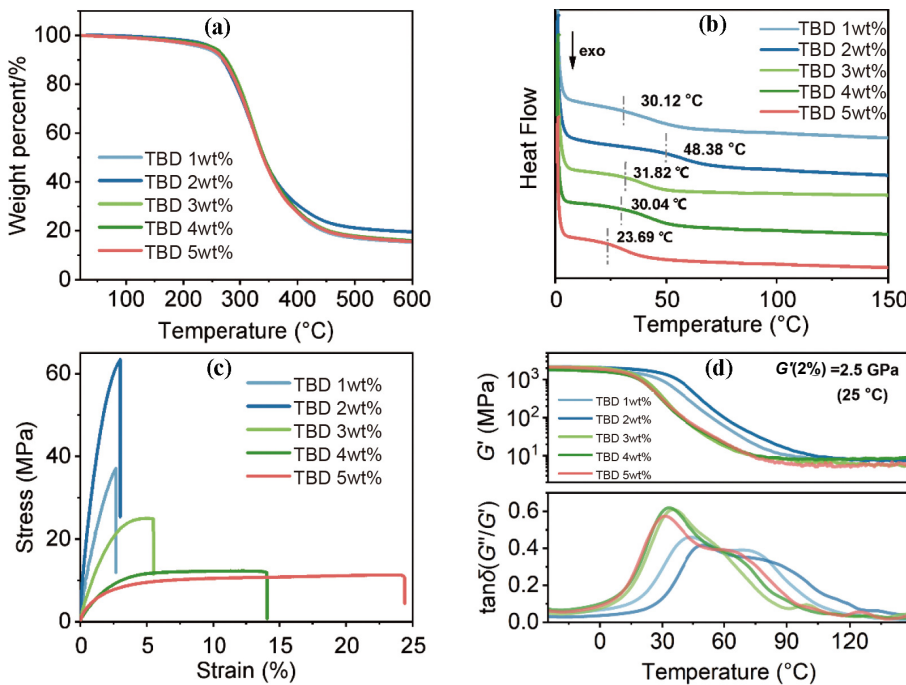


FIG. 4 Thermal and mechanical properties of FEP with different TBD catalyst concentrations ranging from 1 wt% to 5 wt%. (a) TGA cures. (b) DSC curves. (c) Stress-strain curves. (d) Dynamic thermomechanical analysis (DMA) thermal sweep curves. DMA temperature ramp frequency sweep (25 °C to 200 °C, 3 °C·min⁻¹, 15 μm, 1 Hz) results highlighting storage modulus (G' , FIG. 4(d) upper), and $\tan\delta$ (G''/G' , FIG. 4(d) lower).

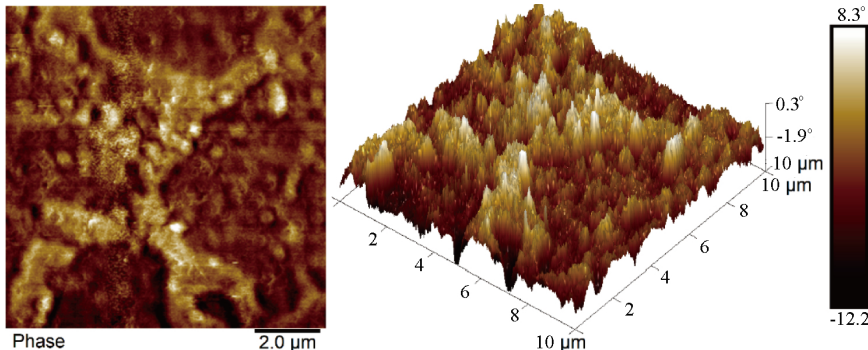


FIG. 5 AFM image for FEP.

ant microstructure.

D. Chemical stability analysis

Through methanol swelling experiments on FEP, the gel fraction and swelling ratio were measured to evaluate the chemical stability of FEP in various solvents, further corroborating its stability during service. As shown in Table II, within the TBD concentration range of 1–5 wt%, the gel fraction consistently exceeded 96%, indicating the fully established cross-linked network of FEP and its high stability. With increasing catalyst concentration, the gel fraction gradually decreased, which is attributable to the catalyst-promoted transesterification between the sample and methanol, leading

TABLE II Gel content and swelling ratio of FEP in methanol under different TBD concentrations.

TBD/wt%	Gel content/%	Swelling ratio/%
1	100.00	8.70
2	98.92	12.19
3	97.22	15.05
4	96.34	15.05
5	96.64	15.72

to a measurable mass loss. This side transesterification with the solvent, though minor, confirms the dynamic nature of the ester bonds even at room temperature when catalyzed. Across all TBD concentrations, the swelling ratio of FEP remained above 8% and increased with higher TBD content, demonstrating that FEP un-

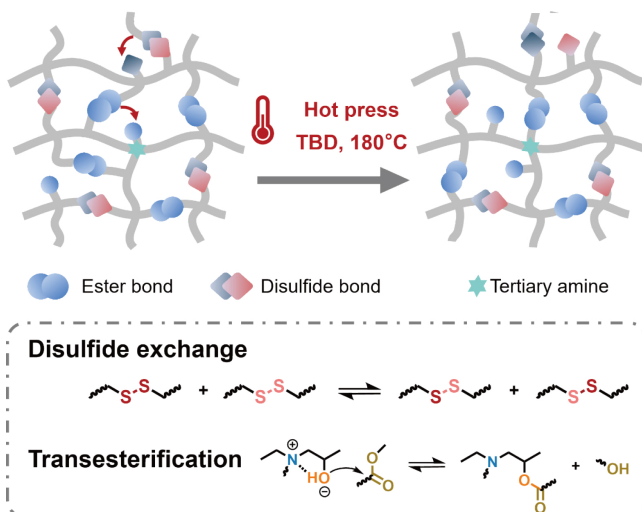


FIG. 6 Hot press rearrangement mechanisms in FEP with 2 wt% TBD.

dergoes swelling without decomposition and further confirming its chemical stability. The increase in swelling ratio with TBD content indicates a slight increase in network mesh size or a decrease in cross-linking density due to the aforementioned side reactions or network rearrangement facilitated by the catalyst, consistent with the mechanical property trends.

E. Hot pressing mechanisms

The dynamic disulfide and ester bonds in FEP are both associative bonds that undergo thermally induced topological rearrangement, enabling the reprocessing and reuse of waste FEP through hot pressing. The schematic diagram and mechanism of dynamic exchange for ester and disulfide bonds are shown in FIG. 6. The results indicated that the Vitrimer network first undergoes disulfide metathesis catalyzed by TBD, accelerating polymer chain segment movement and thereby promoting transesterification (physical effect). Additionally, disulfide bonds act as nucleophiles to facilitate both transesterification and disulfide exchange (chemical effect). Meanwhile, a synergistic non-covalent interaction exists between tertiary amines and TBD, which further promotes transesterification. Specifically, the hydroxyl group adjacent to the tertiary amine is more likely to exchange with intermolecular ester groups rather than intramolecular ones. Due to the electron-donating conjugation effect of the furan rings, the adjacent ester groups are stabilized, resulting in reduced transesterification activity. This allows the Vitrimer network to maintain mechanical integrity dur-

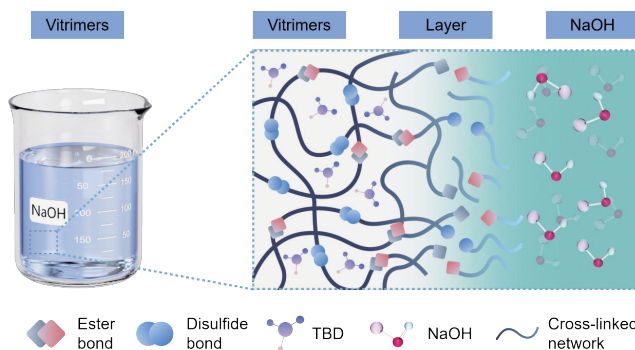


FIG. 7 Schematic diagram of the degradation mechanism of FEP under alkaline conditions (1 mol/L NaOH).

TABLE III The mechanical properties of FEP before and after hot pressing.

Sample	Tensile strength/MPa	Elongation at break/%
Original	64.0	3.0
1 st	62.5	3.0
2 nd	61.8	2.7

ing dynamic exchange. This delicate balance—sufficient activity for network reshuffling under processing conditions yet adequate stability under service conditions—is the hallmark of a well-designed Vitrimer. Ultimately, under processing conditions of 180 °C and 20 MPa, fragmented FEP material was fully restored within 1 h. The hot-pressed samples exhibited excellent recovery of mechanical properties, retaining over 95% of the original tensile strength and more than 90% of the elongation at break (Table III).

F. Chemical degradation mechanism

Closed-loop recyclability is a critical factor in the development of sustainable materials. Under mild alkaline conditions (25 °C, 1 mol/L NaOH), FEP achieves complete degradation within only 4 h (FIG. 7). This behavior originates from the dynamic nature of the disulfide and ester bonds: base-mediated nucleophilic cleavage of the disulfide bonds generates two deprotonated thiol species. Simultaneously, the ester bonds undergo irreversible saponification under alkaline conditions, yielding carboxylate anions and polyols, ultimately forming a homogeneous solution free of ester-bond residues after the reaction is complete. Specifically, the degradation mechanism involved: i) nucleophilic attack by OH⁻ on the carbonyl carbon, leading to the formation of a tetrahedral oxyanion intermediate; ii) collapse of the unstable intermediate, with the alkoxy group (−R'OH) departing as a leaving group, producing carboxylate anions (RCOO⁻) and polyols (R'OH). Quantifi-

TABLE IV Chemical degradation recovery products and recovery rate.

Raw material	Recovered product	Recovery rate/%
Thioctic acid	Thioctic acid	70
Bifunctional epoxide	Polyols	55
Tetrafunctional epoxide	Polyols	55

tatively, this process achieved a high mass recovery rate of 70% to the monomer TA and 55% to polyols (Table IV).

IV. CONCLUSION

In this study, a fully bio-based epoxy Vitrimer FEP featuring a dual-dynamic covalent network was successfully developed. The concentration of the TBD catalyst was identified as a critical factor governing its comprehensive properties. The key findings, categorized by the effect of TBD concentration on specific performance metrics, are summarized as follows:

- (1) Curing kinetics: TBD effectively catalyzed the curing process by lowering the activation energy. The optimal efficiency was achieved at a concentration of 2 wt%, which corresponded to the lowest apparent activation energy ($E_a \approx 47.2 \text{ kJ/mol}$). Both lower and higher concentrations resulted in slower effective curing rates.
- (2) Thermal properties: The glass transition temperature (T_g) was significantly influenced by the catalyst concentration. It reached a maximum of approximately 50 °C at 2 wt% TBD, indicating an optimal cross-linking density and network stability. Deviations from this concentration led to a lower T_g .
- (3) Mechanical properties: The tensile strength and toughness balance was highly dependent on TBD content. The tensile strength (64 MPa) was achieved at 2 wt%, while the elongation at break generally increased with higher catalyst concentrations, demonstrating a tunable strength-toughness profile.
- (4) Recycling performance: The rate of dynamic bond exchange, which governs stress relaxation and reprocessability, was directly accelerated by TBD. At the optimized 2 wt% concentration, FEP demonstrated excellent thermal reprocessability (fully reshaped within 1 h at 180 °C) and complete chemical degradability in mild alkali (1 mol/L NaOH) within 6 h at 25 °C.

In summary, precise tuning of the TBD catalyst concentration to 2 wt% enabled the creation of a sustainable epoxy Vitrimer that successfully integrates robust

mechanical properties, thermal stability, and versatile closed-loop recyclability. This work provides a fundamental understanding of catalyst dosage effects in dual-dynamic network Vitrimers and presents a practical, high-performance material platform capable of addressing the end-of-life challenges of thermoset composites in critical applications like wind energy. Future research will focus on evaluating the long-term stability of this material under simulated service environments, as well as studying the processing and properties of its composites with fiber reinforcements as a matrix resin, to promote its practical application.

V. ACKNOWLEDGEMENTS

The authors gratefully acknowledge the financial support from the National Natural Science Foundation of China (Nos. 22293011, T2341001), the Major Science and Technology Project of Anhui Province (202203a06020010).

- [1] G. M. Scheutz, J. J. Lessard, M. B. Sims, and B. S. Sumerlin, *J. Am. Chem. Soc.* **141**, 16181 (2019).
- [2] C. J. Kloxin, T. F. Scott, B. J. Adzima, and C. N. Bowman, *Macromolecules* **43**, 2643 (2010).
- [3] P. R. Christensen, A. M. Scheuermann, K. E. Loeffler, and B. A. Helms, *Nat. Chem.* **11**, 442 (2019).
- [4] S. Huang, Y. Shen, H. K. Bisoyi, Y. Tao, Z. Liu, M. Wang, H. Yang, and Q. Li, *J. Am. Chem. Soc.* **143**, 12543 (2021).
- [5] C. B. Zhao, L. K. Feng, H. Xie, M. L. Wang, B. Guo, Z. Y. Xue, C. Z. Zhu, and J. Xu, *Chin. J. Polym. Sci.* **42**, 73 (2024).
- [6] D. Montarnal, M. Capelot, F. Tournilhac, and L. Leibler, *Science* **334**, 965 (2011).
- [7] C. Cui, F. Wang, X. Chen, T. Xu, Z. Li, K. Chen, Y. Guo, Y. Cheng, Z. Ge, and Y. Zhang, *Adv. Funct. Mater.* **34**, 2315469 (2024).
- [8] X. Wu, P. Hartmann, D. Berne, M. De Bruyn, F. Cuminet, Z. Wang, J. M. Zechner, A. D. Boese, V. Placet, S. Caillol, and K. Barta, *Science* **384**, eadj9989 (2024).
- [9] Y. Wang, W. Shao, L. Chen, X. Sang, J. Zhou, and J. Wang, *ACS Appl. Polym. Mater.* **7**, 13236 (2025).
- [10] E. K. Bang, M. Lista, G. Sforazzini, N. Sakai, and S. Matile, *Chem. Sci.* **3**, 1752 (2012).
- [11] A. J. Parker and N. Kharasch, *Chem. Rev.* **59**, 583 (1959).
- [12] Y. Liu, Y. Jia, Q. Wu, and J. S. Moore, *J. Am. Chem. Soc.* **141**, 17075 (2019).